Am J Transl Res 2025;17(4):2712-2720
www.ajtr.org /ISSN:1943-8141/AJTR0162322

Original Article

Diagnostic efficiency of peripheral tumor serum biomarkers in lung cancer and their correlation with clinicopathological features

Hongjuan Lv[1*], Ping Luo[1*], Jiahe Wang[1], Chen Chen[1], Yuanyuan Guo[1], Yanhong Li[2]

[1]Department of Respiratory and Critical Care Medicine, The Fourth Hospital of Daqing City, Daqing 163453, Heilongjiang, China; [2]Department of Critical Care Medicine, The Fourth Hospital of Daqing City, Daqing 163453, Heilongjiang, China. [*]Equal contributors.

Received November 28, 2024; Accepted March 31, 2025; Epub April 15, 2025; Published April 30, 2025

Abstract: Objective: To investigate the clinical value of serum tumor markers - carcinoembryonic antigen (CEA), endothelial cell-specific molecule-1 (ESM-1), neuron-specific enolase (NSE), and cytokeratin 19 fragment (CYFRA21-1) - in the diagnosis of lung cancer, and to evaluate the role of preoperative imaging in lung cancer diagnosis. Methods: A total of 56 lung cancer patients, diagnosed at The Fourth Hospital of Daqing City between January 2022 and December 2023, were included in the lung cancer group. Additionally, 69 patients with benign pulmonary tumors diagnosed during the same period were included in the benign tumor group. Preoperative peripheral serum levels of CEA, CYFRA21-1, NSE, and ESM-1 were compared between the two groups. The expression profiles of these biomarkers were further analyzed, focusing on their correlation with TNM staging, lymph node metastasis, and tumor differentiation. Receiver operating characteristic (ROC) curves were plotted to assess the diagnostic performance of these biomarkers. Imaging characteristics were also compared between the two groups to identify features indicative of lung cancer. Results: Serum levels of CYFRA21-1, CEA, ESM-1, and NSE were significantly higher in the lung cancer group compared to the benign tumor group (all $P < 0.05$). Pathological analysis revealed that these markers were notably associated with low to medium tumor differentiation, lymph node metastasis, and advanced stage (III-IV) (all $P < 0.05$). Additionally, small cell lung cancer patients exhibited higher positive rates of CYFRA21-1 and elevated levels of CEA, ESM-1, and NSE compared to non-small cell lung cancer patients. ROC curve analysis demonstrated AUC values of 0.878, 0.778, 0.773, and 0.654 for CYFRA21-1, CEA, ESM-1, and NSE, respectively. Imaging features, including spiculated margins, lobulation, pleural retraction, vascular convergence, vacuolar signs, and larger nodule size, were more prevalent in lung cancer patients and were identified as independent risk factors for lung cancer. Conclusion: Peripheral serum biomarkers, including CYFRA21-1, CEA, ESM-1, and NSE, demonstrate significant diagnostic potential for lung cancer. Furthermore, imaging characteristics provide valuable insights for distinguishing lung cancer, underscoring the clinical applicability of both diagnostic approaches.

Keywords: Lung cancer, serum biomarkers, imaging features, clinical utility, diagnostic performance

Introduction

Lung cancer, a leading malignancy of the respiratory system, represents a significant global health threat and remains one of the most challenging issues in modern medicine [1, 2]. According to the World Health Organization, the global incidence of lung cancer continues to rise, making it one of the primary causes of cancer-related mortality [3, 4]. The incidence of lung cancer, however, is not uniformly distributed; it is influenced by geographic, economic, and cultural factors. In many developing countries, limited economic resources and insufficient healthcare infrastructure hinder early detection and screening efforts, often resulting in diagnoses at more advanced stages, when treatment options are less effective [5]. In contrast, while developed countries benefit from relatively advanced healthcare systems, lung cancer rates remain high due to factors such as fast-paced lifestyles, worsening environmental pollution, and the prevalence of smoking [6]. This disparity highlights the urgent need for

https://doi.org/10.62347/TAEI9443

effective public health strategies to reduce lung cancer incidence and enhance early diagnostic capabilities, making it a global priority for governments and health organizations.

Currently, lung cancer diagnosis relies heavily on histopathological examination; however, its application in large-scale screening is limited due to patient risks. Studies have demonstrated that serum tumor markers, particularly in the early stages of lung cancer, are closely correlated with disease progression and severity, offering a more convenient and rapid diagnostic approach. Among the most widely studied markers are cytokeratin 19 fragment (CYFRA21-1), carcinoembryonic antigen (CEA), neuron-specific enolase (NSE), and endothelial cell-specific molecule-1 (ESM-1). Previous research has shown that abnormal expression of these biomarkers can assist in lung cancer diagnosis. CEA, a glycoprotein, is directly produced by lung cancer cells and is often elevated in the serum of affected individuals. CYFRA21-1, found abundantly in epithelial cells, is typically elevated in the circulation of lung cancer patients. NSE, a product of tumor cell proliferation, is also elevated in the serum of many lung cancer patients. ESM-1, expressed in tumor endothelial cells, promotes tumor progression by facilitating cell proliferation, accelerating angiogenesis, and disrupting normal immune responses [7, 8]. In addition to serum biomarkers, imaging findings play a crucial role in lung cancer diagnosis. However, most studies to date have primarily focused on either serum biomarkers or imaging, leaving certain research gaps unexplored [9, 10]. Therefore, this study analyzed both serum biomarker levels and imaging features of lung cancer patients diagnosed at our center, aiming to identify potential targets for improving early diagnosis.

General information and methods

General information

This study included 56 lung cancer patients diagnosed at The Fourth Hospital of Daqing City between January 2022 and December 2023, who were assigned to the lung cancer group. This study was approved by the Ethics Committee of The Fourth Hospital of Daqing City. Additionally, 69 patients diagnosed with benign pulmonary tumors during the same period were included in the benign tumor group.

To determine the required sample size for this study, we applied the following calculations, which use a parallel 1:1 design to compare the malignant and the benign groups. Based on previous studies evaluating the diagnostic efficacy of hematological indicators for lung nodules, we assumed a diagnostic positive rate of $\mu1 = 0.75$ for the control group and $\mu2 = 0.85$ for the experimental group, with a standard deviation of $\sigma = 0.1$. Considering a 10% dropout rate, an α (Type I error probability) of 0.05, and a statistical power (1-β) of 80%, the required sample size was calculated using the following formula for clinical trial sample size estimation:

$$n1 = n2 = \frac{2 (Z_{\alpha/2} + Z_{\beta})^2 \times \sigma^2}{(\mu1 - \mu2)^2}$$

Substituting the parameters ($\mu1 = 0.75$, $\mu2 = 0.85$, $\sigma = 1$, $\alpha = 0.05$, and $\beta = 0.2$), the calculation yielded $n1 = n2 = 12$. Consequently, the minimum sample size required for this study was 24 patients. To enhance the robustness and reliability of the study results, we selected all patients who met the inclusion criteria during the study period, resulting in a final cohort of 115 patients.

Inclusion criteria

(1) Patients with pulmonary nodules detected by preoperative chest CT who subsequently underwent surgical resection. (2) Common imaging features of pulmonary nodules, including spiculated margins, calcification, satellite lesions, pleural retraction, lobulation, and vascular signs. (3) Patients with complete medical records, including current and past medical histories, as well as preoperative laboratory and imaging results. (4) First-time visitors diagnosed with pulmonary nodules.

Exclusion criteria

(1) Patients with tumors of other organs, such as those in the digestive or hematologic systems, identified during preoperative examinations. (2) Patients with multiple pulmonary nodules on chest CT, where the underlying pathology cannot be determined. (3) Patients with congenital pulmonary structural abnormalities. (4) Patients with severe organ dysfunction, such as heart or kidney failure. (5) Patients with

Table 1. Comparison of baseline data between the two groups

Items	Lung cancer group (n = 56)	Benign group (n = 69)	Statistical value	P
Gender (Male/female)	35/21	45/24	0.099	0.753
Age	47.8 ± 5.3	48.1 ± 5.4	-0.311	0.756
BMI	24.2 ± 2.6	23.9 ± 2.7	0.628	0.531
Hypertension	11	14	0.293	0.588
Nodule distribution (left/right)	30/26	42/27	0.674	0.411
Nodule discovery time (years)	3.9 ± 0.5	3.8 ± 0.6	0.997	0.321

Note: BMI: body mass index.

mental disorders or communication impairments that hinder effective interaction. (6) Patients with incomplete clinical data.

Data acquisition

Data were collected through a comprehensive review of electronic medical records, which included patient baseline characteristics, blood test results, and CT images. Fasting blood samples were obtained for the measurement of serum levels of CEA, CYFRA21-1, NSE, and ESM-1. Biochemical indicators in the morning are relatively stable, providing a more reliable basis for subsequent analysis. Fasting peripheral venous blood (3-5 ml) was collected from all participants on the morning after admission. The samples were then centrifuged at 3000 rmp for 20 minutes, and the supernatant serum was collected for testing. Serum levels of the markers were measured using electrochemiluminescence or enzyme-linked immunosorbent assay (ELISA) methods, with reagent kits purchased from Roche Diagnostics (Shanghai). All procedures were strictly followed according to the manufacturer's instructions.

The primary indicators were determined based on the gold standard for lung cancer diagnosis, which includes obtaining lung tissue samples for pathological examination, evaluating tissue morphology, and performing staining and immunohistochemical analyses to determine the pathological classification of lung nodules. The diagnostic efficacy of imaging features and serum markers for detecting pulmonary malignancies was then compared [11].

Secondary observational indicators: Secondary indicators involved the comparison of peripheral blood test results between the malignant and benign groups, including routine blood tests, such as white blood cell count (reflecting immune system status), liver function tests (e.g., transaminases: alanine aminotransferase (ALT), aspartate aminotransferase (AST)), and kidney function markers (e.g., creatinine, blood urea nitrogen). The goal was to explore the differences in the expression of these hematological indicators between lung cancer patients and healthy individuals.

Data analysis

Data were analyzed using SPSS 22.0 software. Measurement data were expressed as mean ± SEM. For normally distributed data, t-tests were performed, with paired t-tests for within-group comparisons and independent samples t-tests for between-group comparisons. For non-normally distributed data, the Mann-Whitney U test was used. Categorical data were expressed as frequencies (percentages), and the chi-square (χ^2) test was applied for their analysis. Variables with statistically significant differences in univariate analyses were included in a logistic regression model to calculate the odds ratio (OR) and its 95% confidence interval (CI). The receiver operating characteristic (ROC) curve of the subjects was used to analyze the diagnostic value of serological indicators for lung cancer. A p-value of < 0.05 was considered statistically significant.

Results

Comparison of baseline data between malignant and benign groups

The results showed no statistically significant differences between the two groups in terms of sex, age, body mass index (BMI), nodule distribution, or nodule discovery time, indicating the two groups were comparable (**Table 1**).

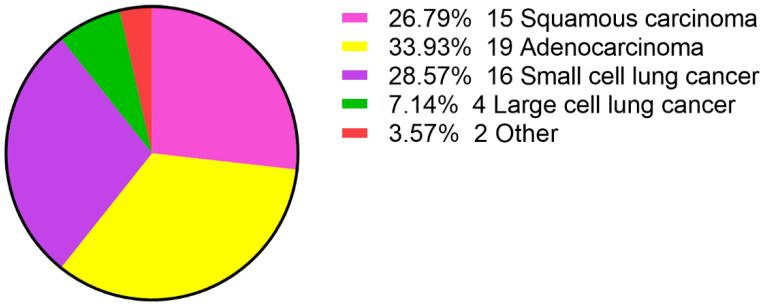

Figure 1. Pathological classification of lung cancer patients in the lung cancer group.

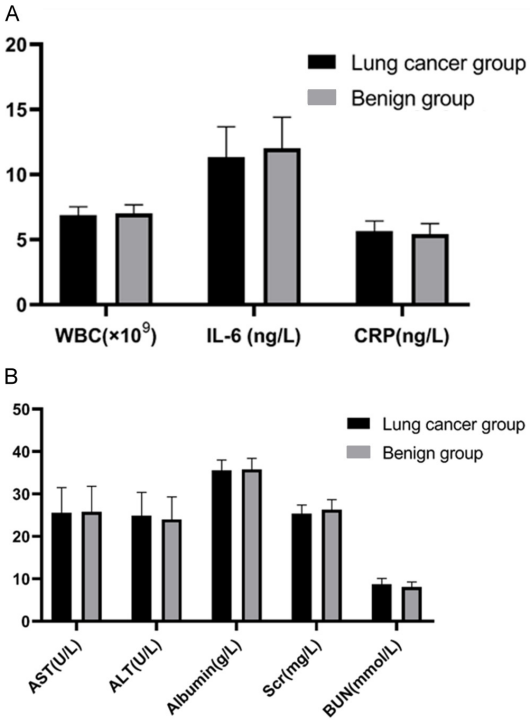

Figure 2. Comparison of inflammatory markers, and liver and kidney function between the two groups. A. Comparison of inflammatory markers between the two groups; B. Comparison of liver and kidney function between the two groups. WBC: white blood cell count, IL-6: interleukin-6, CRP: C-reactive protein, AST: aspartate aminotransferase, ALT: alanine aminotransferase, ALB: albumin, SCR: serum creatinine, BUN: blood urea nitrogen.

Final pathological results of 56 malignant patients

Among the 56 lung cancer patients included in the study, the predominant histological types were adenocarcinoma, small cell lung cancer, and squamous cell carcinoma, followed by large cell lung cancer and other less common types. The distribution and composition of lung cancer subtypes are summarized in **Figure 1**.

Comparison of peripheral blood inflammatory markers and liver and kidney function between the two groups

No statistically significant differences were observed between the two groups in terms of white blood cell count (WBC) (6.89 ± 1.76 × 10^9 vs. 7.02 ± 1.75 × 10^9), serum C-reactive protein (CRP) (11.76 ± 2.00 vs. 12.44 ± 1.87), and interleukin-6 (IL-6) levels (5.00 ± 1.03 vs. 5.88 ± 1.14) (all $P > 0.05$), as shown in **Figure 2A**. Additionally, no significant differences were found in liver function markers, including ALT (25.6 ± 6.7 vs. 26.0 ± 6.6), AST (25.4 ± 6.4 vs. 24.9 ± 5.4) and albumin (ALB) (38.9 ± 3.4 vs. 39.0 ± 3.5), or in renal function markers, such as serum creatinine (SCR) (26.7 ± 4.3 vs. 27.0 ± 4.1), BUN (8.67 ± 0.45 vs. 8.00 ± 0.43), between the two groups (**Figure 2B**).

Comparison of peripheral blood CEA, CYFRA21-1, NSE, and ESM-1 levels between the two groups

Peripheral blood levels of CEA (36.23 ± 7.68 vs. 18.47 ± 6.54), CYFRA21-1 (11.25 ± 2.80 vs. 6.56 ± 2.61), NSE (32.55 ± 2.38 vs. 21.87 ± 3.24), and ESM-1 (49.34 ± 8.7 vs. 28.76 ± 5.3) were significantly higher in the lung cancer group compared to the benign group (all $P < 0.05$) (**Table 2**).

Comparison of peripheral blood CEA, CYFRA21-1, NSE, and ESM-1 levels between small cell lung cancer and non-small cell lung cancer patients

The results showed that peripheral blood levels of CEA, CYFRA21-1, NSE, and ESM-1 were significantly higher in small cell lung cancer patients compared to non-small cell lung cancer patients (all $P < 0.05$) (**Table 3**).

Diagnostic efficacy of peripheral blood CEA, CYFRA21-1, NSE, and ESM-1 for lung cancer

The diagnostic efficacy of peripheral blood CEA, CYFRA21-1, NSE, and ESM-1, as measured by

Table 2. Comparison of peripheral blood levels of CEA, CYFRA21-1, NSE and ESM-1 between the two groups

Items	Lung cancer group (n = 56)	Benign group (n = 69)	t	P
CEA (ng/ml)	36.23 ± 7.68	18.47 ± 6.54	13.962	< 0.001
CYFRA21-1 (ng/ml)	11.25 ± 2.80	6.56 ± 2.61	9.670	< 0.001
NSE (ng/ml)	32.55 ± 2.38	21.87 ± 3.24	20.566	< 0.001
ESM-1 (ng/ml)	49.34 ± 8.70	28.76 ± 5.30	16.284	< 0.001

Note: CEA: carcinoembryonic antigen, CYFRA21-1: cytokeratin 19 fragment, NSE: neuron-specific enolase, ESM-1: endothelial cell-specific molecule-1.

Table 3. Comparison of peripheral blood levels of CEA, CYFRA21-1, NSE and ESM-1 between patients with different types of lung cancer

Items	Small cell lung cancer (n = 48)	Non-small cell lung cancer (n = 18)	t	P
CEA (ng/ml)	58.17 ± 6.57	24.38 ± 5.43	31.486	< 0.001
CYFRA21-1 (ng/ml)	13.16 ± 2.79	8.47 ± 2.50	9.901	< 0.001
NSE (ng/ml)	46.43 ± 2.27	28.79 ± 3.15	35.140	< 0.001
ESM-1 (ng/ml)	68.24 ± 7.60	34.68 ± 5.40	28.809	< 0.001

Note: CEA: carcinoembryonic antigen, CYFRA21-1: cytokeratin 19 fragment, NSE: neuron-specific enolase, ESM-1: endothelial cell-specific molecule-1.

the area under the ROC curve (AUC), was 0.910, 0.875, 0.797, and 0.871, respectively. These findings indicate the strong diagnostic potential of these biomarkers for lung cancer (**Table 4** and **Figure 3**).

Univariate analysis of lung cancer imaging features

Significant differences were observed between lung cancer patients and those with benign lesions in several imaging features, including spiculation, lobulation, pleural retraction, vascular convergence, vacuole formation, and nodule size. Multivariate analysis confirmed that these features were independent risk factors for the malignant transformation of pulmonary nodules. Detailed results are presented in **Tables 5**, **6**.

Serum tumor marker levels in lung cancer patients with different pathological features

The study found that lung cancer patients with low to moderate differentiation, lymph node metastasis, and advanced stages (III-IV) exhibited markedly higher levels of serum tumor markers (**Table 7**).

Discussion

Recent studies have shown a significant and ongoing increase in the incidence of lung cancer, a malignant respiratory tumor, making it one of the most prevalent cancers globally [12-14]. According to statistics from the World Health Organization, lung cancer has surpassed other cancers as the leading cause of cancer-related deaths. However, in clinical practice, many patients are diagnosed at advanced stages due to the late onset of symptoms or the presence of conditions such as pulmonary infections, shortness of breath, and chest tightness. Consequently, fewer than 30% of patients are eligible for surgery at the time of diagnosis [15, 16]. Thus, early and effective diagnosis is crucial for improving patient prognosis.

Currently, the diagnosis of lung cancer primarily relies on histopathological examination of tissue samples obtained via surgery or biopsy. However, many patients diagnosed with lung cancer are not immediately eligible for surgery, emphasizing the importance of early detection. Tumor markers, the biological molecules produced either by tumor cells or within the tumor microenvironment, can be detected in blood, urine, or other body fluids. Their presence is closely associated with cancer development and progression, providing valuable diagnostic information for clinicians [17]. Therefore, this study retrospectively analyzed data from lung cancer patients at our center, along with their serum biomarker levels, to assess the diagnos-

Table 4. Diagnostic efficacy of CEA, CYFRA21-1, NSE and ESM-1 for lung cancer

Items	AUC	95% CI	Sensitivity	Specificity
CEA	0.910	0.859-0.960	0.667	0.841
CYFRA21-1	0.875	0.816-0.934	0.686	0.794
NSE	0.797	0.709-0.885	0.704	0.884
ESM-1	0.871	0.811-0.932	0.734	0.781

Note: CEA: carcinoembryonic antigen, CYFRA21-1: cytokeratin 19 fragment, NSE: neuron-specific enolase, ESM-1: endothelial cell-specific molecule-1.

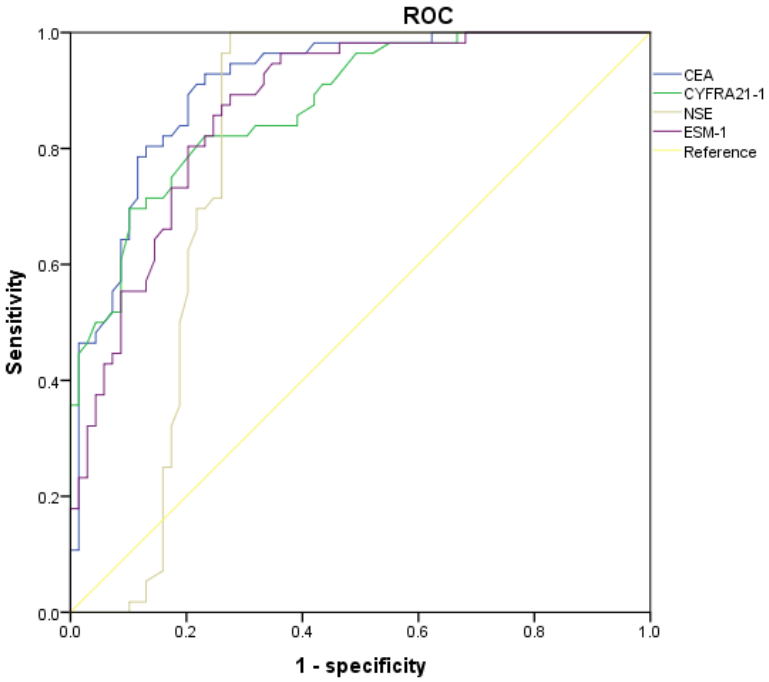

Figure 3. AUC in peripheral blood. CEA: carcinoembryonic antigen, CYFRA21-1: cytokeratin 19 fragment, NSE: neuron-specific enolase, ESM-1: endothelial cell-specific molecule-1.

tic and prognostic value of CEA, CYFRA21-1, NSE, and ESM-1.

Previous studies have shown that the levels of CEA, CYFRA21-1, NSE, and ESM-1 in the peripheral blood of lung cancer patients are significantly higher than those in healthy controls [17]. The mechanisms underlying these elevated levels are as follows: CEA, a high-molecular-weight glycoprotein, is directly produced by lung cancer cells, and is primarily used as a tumor marker for non-small cell lung cancer. CYFRA21-1, a differentiation-specific protein, is widely distributed in epithelial cells and constitutes part of the cytoskeleton. During the malignant transformation of epithelial cells, activated proteases accelerate keratin degradation, releasing a large number of keratin fragments into the bloodstream, which are typically abundant in lung cancer patients. Furthermore, NSE is an enzyme involved in glycolysis, and its elevated levels may result from the high proliferative activity of tumor cells, leading to increased inflammatory responses in surrounding tissues. Finally, ESM-1, a dermatan sulfate proteoglycan secreted by activated vascular endothelial cells, serves as a marker of endothelial dysfunction and cell proliferation. It plays a critical role in the development and progression of lung cancer by promoting cell proliferation, enhancing angiogenesis, and contributing to immunosuppression within the tumor microenvironment [18-20]. In addition, we observed that the levels of CEA, CYFRA21-1, NSE, and ESM-1 in the peripheral blood of small cell lung cancer patients were higher than those in non-small cell lung cancer patients. This may be attributed to the higher malignancy of small cell lung cancer, which supports the conclusions of previous studies [21, 22].

Moreover, previous imaging studies have confirmed that several radiological features of lung lesions play a crucial role in determining whether a tumor is benign or malignant [23, 24]. In the current analysis of imaging data for both benign and malignant lung nodules, significant differences were observed between the two groups in terms of features such as spiculated margins, lobulation, pleural retraction, vascular convergence, vacuolar signs, size, calcification, and satellite lesions. Logistic regression analysis identified these features as independent predictors of lung nodule

Table 5. Univariate analysis of malignant transformation of pulmonary nodules

CT signs	Benign group (n = 56)	Lung cancer group (n = 69)	F/χ^2	*P*
Spiculated sign	13	25	7.430	0.006
Lobulated sign	11	29	5.110	0.024
Pleural traction sign	10	31	7.518	0.006
Vascular convergence sign	13	32	5.173	0.023
Cavitary sign	20	49	8.416	0.004
Nodule diameter			3.860	0.049
> 1 cm	12	26		
≤ 1 cm	44	43		
Calcification	30	19	8.791	0.003
Satellite lesions	20	40	6.135	0.013

Table 6. Multivariate logistic regression analysis of malignant transformation of pulmonary nodules

Variable	Standardized β	OR	95% CI	P
Spiculated sign	0.775	3.37	1.58-7.78	0.029
Lobulated sign	0.658	3.03	1.27-6.37	0.027
Pleural traction sign	0.469	4.38	1.04-5.38	0.021
Vascular convergence sign	0.479	3.05	1.09-8.36	0.022
Cavitary sign	0.657	3.84	1.16-9.02	0.035
Nodule diameter > 1.0 cm	0.958	4.89	1.04-8.70	0.001
Calcification	-3.034	0.58	0.31-0.75	0.036
Satellite lesions	-4.239	0.74	0.53-0.89	0.003

Table 7. Comparison of tumor markers in lung cancer patients with different pathological characteristics

Biomarker	Degree of differentiation		Lymph node metastasis		TNM staging	
	Low/medium differentiation	High differentiation	Yes	No	Stage I-II	Stage III-IV
CEA (ng/ml)	78.17 ± 4.57	45.28 ± 5.07*	80.40 ± 18.72	37.54 ± 16.43*	39.03 ± 14.51	73.45 ± 15.06*
CYFRA21-1 (ng/ml)	18.07 ± 2.68	12.34 ± 1.57*	20.57 ± 3.41	11.89 ± 2.06*	12.76 ± 3.08	25.64 ± 4.55*
NSE (ng/ml)	68.24 ± 5.67	30.62 ± 4.34*	71.60 ± 6.50	34.56 ± 7.80*	43.78 ± 9.07	83.57 ± 11.25*
ESM-1 (ng/ml)	78.23 ± 8.04	55.48 ± 7.69*	89.52 ± 7.34	60.03 ± 8.11*	95.34 ± 9.51	65.01 ± 10.33*

Note: CEA: carcinoembryonic antigen, CYFRA21-1: cytokeratin 19 fragment, NSE: neuron-specific enolase, ESM-1: endothelial cell-specific molecule-1. *: $P < 0.05$.

malignancy, with calcification and satellite lesions found to be protective factors. Spiculated margins often result from tumor cell infiltration into surrounding tissues. This infiltration typically occurs through the invasion of adjacent bronchovascular sheaths or local lymphatic vessels, a process that involves cell motility and complex signaling between cells, as well as alterations in the extracellular matrix. The presence of lobulation indicates that tumor cells have invaded surrounding tissues, signifying growth and dissemination. Pleural retraction occurs when the tumor invades the pleura, with bioactive substances secreted by tumor cells stimulating the pleura tissue, thereby triggering an inflammatory response and leading to pleural traction. The vascular convergence sign, manifested by thickened vascular structures, is often a result of the tumor's rapid growth, which requires an increased blood supply. The vacuolar sign, observed as small low-density areas (1-3 mm in diameter) within the lung, indicates residual aerated lung tissue or bronchi forming a mass, with air-filled spaces appearing as low-density regions. The size of a lung nodule is directly related to its

likelihood of malignancy, with nodules lager than 1 cm in diameter being more likely to be malignant due to their faster growth compared to benign lesions. Additionally, this study shows that calcification and satellite lesions may act as protective factors against the malignant transformation of lung nodules. Calcification is typically observed in nodules resulting from prior lung infections, such as tuberculosis or fungal infections, or as a consequence of chronic inflammatory reactions. Therefore, post-inflammatory nodules are generally benign. Satellite lesions, smaller nodules located within a lung lobe, are often associated with infections or inflammation. These lesions, typically appearing as small nodules surrounding a larger nodule, often suggest that the larger nodule is benign. These findings are consistent with conclusions drawn in previous studies [25, 26].

Conclusion

Peripheral blood levels of CEA, CYFRA21-1, NSE, and ESM-1 are closely associated with the occurrence of lung cancer. Their combined use in diagnostic practice enhances the detection rate of lung cancer and provides significant diagnostic value, supporting their clinical utility. However, this study has several limitations, including a relatively small sample size and a single-center design. Additionally, the variation in the severity of patient conditions, along with the nested nature of the cases, underscores the need for further validation through multicenter, large-scale studies. Furthermore, this study did not evaluate the combined diagnostic efficacy of these biomarkers for liver cancer, as each marker showed better individual diagnostic performance for lung cancer. Therefore, exploring the potential combined predictive value of these markers remains a key area for future research. Finally, the follow-up period in this study was relatively short, and additional longitudinal studies are needed to further clarify the role of these serum biomarkers in predicting the long-term prognosis of lung cancer patients.

Disclosure of conflict of interest

None.

Address correspondence to: Yanhong Li, Department of Critical Care Medicine, The Fourth Hospital of Daqing City, No. 198 Central Street, Ranghu District, Daqing 163453, Heilongjiang, China. Tel: +86-13936805990; E-mail: liyanhong_edu@126.com; Yuanyuan Guo, Department of Respiratory and Critical Care Medicine, The Fourth Hospital of Daqing City, No. 198 Central Street, Ranghu District, Daqing 163453, Heilongjiang, China. Tel: +86-13936835010; E-mail: 3265998243@qq.com

References

[1] Li Y, Yan B and He S. Advances and challenges in the treatment of lung cancer. Biomed Pharmacother 2023; 169: 115891.
[2] Abu Rous F, Singhi EK, Sridhar A, Faisal MS and Desai A. Lung cancer treatment advances in 2022. Cancer Invest 2023; 41: 12-24.
[3] Leiter A, Veluswamy RR and Wisnivesky JP. The global burden of lung cancer: current status and future trends. Nat Rev Clin Oncol 2023; 20: 624-639.
[4] Zhang Y, Vaccarella S, Morgan E, Li M, Etxeberria J, Chokunonga E, Manraj SS, Kamate B, Omonisi A and Bray F. Global variations in lung cancer incidence by histological subtype in 2020: a population-based study. Lancet Oncol 2023; 24: 1206-1218.
[5] Han B, Zheng R, Zeng H, Wang S, Sun K, Chen R, Li L, Wei W and He J. Cancer incidence and mortality in China, 2022. J Natl Cancer Cent 2024; 4: 47-53.
[6] Nooreldeen R and Bach H. Current and future development in lung cancer diagnosis. Int J Mol Sci 2021; 22: 8661.
[7] Pei Q, Luo Y, Chen Y, Li J, Xie D and Ye T. Artificial intelligence in clinical applications for lung cancer: diagnosis, treatment and prognosis. Clin Chem Lab Med 2022; 60: 1974-1983.
[8] Lee E and Kazerooni EA. Lung cancer screening. Semin Respir Crit Care Med 2022; 43: 839-850.
[9] Bi H, Yin L, Fang W, Song S, Wu S and Shen J. Association of CEA, NSE, CYFRA 21-1, SCC-Ag, and ProGRP with clinicopathological characteristics and chemotherapeutic outcomes of lung cancer. Lab Med 2023; 54: 372-379.
[10] Wu LH, Chen L, Wang QY and Wang YT. Correlation between HRCT signs and levels of CA125, SCCA, and NSE for different pathological types of lung cancer. Eur Rev Med Pharmacol Sci 2023; 27: 4162-4168.
[11] Liu QX, Zhou D, Han TC, Lu X, Hou B, Li MY, Yang GX, Li QY, Pei ZH, Hong YY, Zhang YX, Chen WZ, Zheng H, He J and Dai JG. A noninvasive multianalytical approach for lung cancer diagnosis of patients with pulmonary nodules. Adv Sci (Weinh) 2021; 8: 2100104.
[12] Li C, Lei S, Ding L, Xu Y, Wu X, Wang H, Zhang Z, Gao T, Zhang Y and Li L. Global burden and

trends of lung cancer incidence and mortality. Chin Med J (Engl) 2023; 136: 1583-1590.
[13] Barta JA, Powell CA and Wisnivesky JP. Global epidemiology of lung cancer. Ann Glob Health 2019; 85: 8.
[14] Oliver AL. Lung cancer: epidemiology and screening. Surg Clin North Am 2022; 102: 335-344.
[15] Lee NY, Hum M, Zihara S, Wang L, Myint MK, Lim DW, Toh CK, Skanderup A, Samol J, Tan MH, Ang P, Lee SC, Tan EH, Lai GGY, Tan DSW, Yap YS and Lee ASG. Landscape of germline pathogenic variants in patients with dual primary breast and lung cancer. Hum Genomics 2023; 17: 66.
[16] Benusiglio PR, Fallet V, Sanchis-Borja M, Coulet F and Cadranel J. Lung cancer is also a hereditary disease. Eur Respir Rev 2021; 30: 210045.
[17] Villalobos P and Wistuba II. Lung cancer biomarkers. Hematol Oncol Clin North Am 2017; 31: 13-29.
[18] Cheng C, Yang Y, Yang W, Wang D and Yao C. The diagnostic value of CEA for lung cancer-related malignant pleural effusion in China: a meta-analysis. Expert Rev Respir Med 2022; 16: 99-108.
[19] Wu LH, Chen L, Wang QY and Wang YT. Correlation between HRCT signs and levels of CA125, SCCA, and NSE for different pathological types of lung cancer. Eur Rev Med Pharmacol Sci 2023; 27: 4162-4168.
[20] Fu L, Wang R, Yin L, Shang X, Zhang R and Zhang P. CYFRA21-1 tests in the diagnosis of non-small cell lung cancer: a meta-analysis. Int J Biol Markers 2019; 34: 251-261.
[21] Li J, Chen Y, Wang X, Wang C and Xiao M. The value of combined detection of CEA, CYFRA21-1, SCC-Ag, and pro-GRP in the differential diagnosis of lung cancer. Transl Cancer Res 2021; 10: 1900-1906.
[22] Yuan J, Sun Y, Wang K, Wang Z, Li D, Fan M, Bu X, Chen J, Wu Z, Geng H, Wu J, Xu Y, Chen M and Ren H. Development and validation of reassigned CEA, CYFRA21-1 and NSE-based models for lung cancer diagnosis and prognosis prediction. BMC Cancer 2022; 22: 686.
[23] Bade BC and Dela Cruz CS. Lung cancer 2020: epidemiology, etiology, and prevention. Clin Chest Med 2020; 41: 1-24.
[24] Panunzio A and Sartori P. Lung cancer and radiological imaging. Curr Radiopharm 2020; 13: 238-242.
[25] Rivera GA and Wakelee H. Lung cancer in never smokers. Adv Exp Med Biol 2016; 893: 43-57.
[26] Thandra KC, Barsouk A, Saginala K, Aluru JS and Barsouk A. Epidemiology of lung cancer. Contemp Oncol (Pozn) 2021; 25: 45-52.